Crystallization Behavior of Poly(ε-caprolactone)/Layered Double Hydroxide Nanocomposites

Zhe Yang, Hongdan Peng, Weizhi Wang, Tianxi Liu

Key Laboratory of Molecular Engineering of Polymers (Ministry of Education), Department of Macromolecular Science, Laboratory of Advanced Materials, Fudan University, Shanghai 200433, People's Republic of China

Received 21 July 2009; accepted 8 November 2009
DOI 10.1002/app.31787
Published online 27 January 2010 in Wiley InterScience (www.interscience.wiley.com).

ABSTRACT: Poly(ε-caprolactone) (PCL)/layered double hydroxide (LDH) nanocomposites were prepared successfully via simple solution intercalation. The nonisothermal melt crystallization kinetics of neat PCL and its LDH nanocomposites was investigated with the Ozawa, Avrami, and combined Avrami–Ozawa methods. The Ozawa method failed to describe the crystallization kinetics of the studied systems. The Avrami method was found to be useful for describing the nonisothermal crystallization behavior, but the parameters in this method do not have explicit meaning for nonisothermal crystallization. The combined Avrami–Ozawa method explained the nonisothermal crystallization behavior of PCL and its LDH nanocomposites effectively. The kinetic results and polarized optical microscopy observations indicated that the addition of LDH could affect the mechanism of nucleation and growth of the PCL matrix. The Takhor model was used to analyze the activation energies of nonisothermal crystallization. © 2010 Wiley Periodicals, Inc. J Appl Polym Sci 116: 2658–2667, 2010

Key words: crystallization; nanocomposites; morphology; poly(ε-caprolactone)

INTRODUCTION

Polymer/inorganic layered material nanocomposites are a class of composites in which at least one dimension of the inorganic phase is on a nanometer scale. These nanocomposites have attracted much research and industrial interest because they often exhibit dramatically enhanced mechanical performance, thermal stability, flame retardancy, and gas-barrier properties.[1–3] However, the majority of the research work has been focused on cationic clays, such as the montmorillonite systems, whereas the layered double hydroxide (LDH) systems have rarely been reported in the literature. LDHs, known as anionic clays or hydrotalcite clays, can be expressed as the following general formula:

$$[M^{II}_{1-x}M^{III}_{x}(OH)_2] \cdot [A^{n-}_{x/n} \cdot mH_2O],$$

where M^{II}_{1-x} and M^{III}_{x} represent divalent and trivalent metal ions, respectively, within the brucite-like layers, and A^{n-} is an interlayer anion.[4] In contrast to layered clays, LDH particles, being composed of metal hydroxide layers, display a positive surface charge, which is counterbalanced by anions located in the domains between adjacent layers. The materials can accommodate a wide range of different anions and cations, and this leads to a large variety of compositions and thus tunability for a large number of applications.[5] In addition, the high aspect ratio of LDH, which is similar to that of montmorillonite, makes it suitable for the fabrication of polymer nanocomposite.[6] Some polymer/LDH nanocomposites have been reported (e.g., polystyrene,[7] polyethylene,[8] nylon 6,[6] and other polymer matrices).

As one of the most important biocompatible and biodegradable aliphatic polyesters, poly(ε-caprolactone) (PCL) has many potential biomedical and packing applications, such as matrices for bone substitutes, scaffolds, drug carriers for controlled release, disposable food service items, and food packing.[9–12] However, the applications of such polymers are limited because of their deficient mechanical and barrier properties with respect to water and gases. It is thought that PCL/LDH nanocomposites will widen the applications of biodegradable polymers as biomedical materials.

In fact, there have been few reports up to now about PCL/LDH nanocomposites.[9,13–17] Vittoria et al.[14] reported the preparation of intercalated PCL nanocomposites reinforced by 12-hydroxydodecanoate anion modified MgAl–LDH (MgAl–LDH–HD). Actually, none of the preparation approaches

Correspondence to: T. Liu (txliu@fudan.edu.cn).
Contract grant sponsor: National Natural Science Foundation of China; contract grant number: 50873027.
Contract grant sponsor: Fudan's Undergraduate Research Opportunities Program (through the Wangdao project); contract grant number: 08093.
Contract grant sponsor: Shanghai Leading Academic Discipline Project; contract grant number: B113.

previously reported, such as the direct melt blending of PCL with MgAl–LDH–HD, the *in situ* polymerization of ε-caprolactone in the presence of MgAl–LDH–HD, and the mixing of a tetrahydrofuran solution of PCL with MgAl–LDH–HD, can successfully achieve exfoliated PCL/LDH nanocomposites because the MgAl–LDH–HD microcrystals remain essentially integrated within the polymeric matrix.[13] In our work, highly exfoliated CoAl–LDH/PCL nanocomposites were successfully obtained by simple refluxing of a mixture of dodecyl sulfate modified CoAl–LDH and PCL in a cyclohexanone solution.[18]

The study of the nonisothermal crystallization of polymers is of great technical importance because most practical processing techniques proceed under nonisothermal conditions.[19] The nonisothermal crystallization behavior of many composite systems including PCL, such as PCL/multiwalled carbon nanotube,[20] PCL/attapulgite,[21] PCL/graphite oxide,[22] and PCL/montmorillonite nanocomposites,[23] has been extensively reported in the literature. For the PCL/LDH nanocomposite system, nonisothermal crystallization behavior has also been investigated. Vittoria et al.[15] studied the isothermal and nonisothermal crystallization behavior of PCL/MgAl–LDH nanocomposites. The Avrami and Tobin methods were used in their study to analyze the nonisothermal crystallization behavior. They concluded that LDH nanolayers had a nucleation effect and affected the growth of the crystallization process of the PCL chains. Here, for the first time, the effect of surfactant-modified CoAl–LDH nanoparticles on the nonisothermal crystallization of PCL was investigated in detail. The purpose of this study was to obtain an extensive understanding of the crystallization behavior of LDH-nanoparticle-filled PCL nanocomposites.

EXPERIMENTAL

Materials

PCL (number-average molecular weight = 80,000 Da; Aldrich, Milwaukee, WI), $CoCl_2 \cdot 6H_2O$, (Sinopharm Chemical Reagent Company, Shanghai, China), $AlCl_3 \cdot 6H_2O$, and urea (analytical purity; Yixing No.2 Chemical Reagent Company, Yixing, China) were supplied by Shanghai Zhenxing Chemicals (Shanghai, China). Sodium dodecyl sulfate, NaCl, and cyclohexanone (analytical purity) were obtained from the China Medicine Group of Shanghai Chemical Reagent Co. (Shanghai, China). All chemicals were used as received without further purification.

Sample preparation

Dodecyl sulfate modified CoAl–LDH was obtained according to a procedure reported previously.[23] The PCL/LDH nanocomposites were prepared by the solution intercalation method. First, the desired amount of LDH was sonicated for 0.5 h and refluxed in 50 mL of cyclohexanone for 12 h under flowing nitrogen. Subsequently, this solution was added to the PCL solution in 50 mL of cyclohexanone, and the solution was refluxed for another 12 h. Finally, the solution was poured into 300 mL of cooled methanol. The precipitates, PCL/LDH nanocomposites, were filtered and dried *in vacuo* at 40°C for 48 h. The products were then molded in a hot press at 100°C, and this was followed by a quick quenching in an ice–water bath. Film samples (with a thickness of ca. 0.5 mm) were obtained and analyzed. The preparation conditions were the same as those for neat PCL and its nanocomposites containing 1, 2, or 4 wt % LDH.

Characterization

Differential scanning calorimetry (DSC) experiments were performed in a nitrogen environment with a Pyris 1 differential scanning calorimeter (Perkin-Elmer, Norwalk, CT). The temperature and heat of fusion were calibrated with the standard procedures. To study the nonisothermal crystallization behavior, each sample was first heated to 100°C at a scanning rate of 10°C/min, maintained there for 3 min to diminish the influence of the previous thermal history, and then cooled to 0°C at four preset cooling rates of 5, 10, 15, and 20°C/min. The crystallization exotherm traces were recorded to study the nonisothermal crystallization kinetics.

The crystalline morphologies of neat PCL and PCL/LDH nanocomposite samples were observed with an Olympus BX-51 polarized optical microscope (Tokyo, Japan) with a Linkam THMS 600 hot stage. The temperature of the hot stage was kept constant within an error of ±0.1°C, and nitrogen gas was purged during measurements. The samples for polarized optical microscopy (POM) observations were prepared by being melted and squeezed into films. These films were kept in the hot stage between two microscope slides, and each sample was heated to 100°C and kept there for 5 min to erase its thermal history. Samples were subsequently cooled to room temperature at a cooling rate of 20°C/min, and then the spherulitic morphology that formed during the nonisothermal crystallization process was observed with POM.

RESULTS AND DISCUSSION

Nonisothermal crystallization behavior

The crystallization behavior of PCL and PCL/LDH nanocomposites was studied at cooling rates between 5 and 20°C/min. Figure 1(a,b) shows the

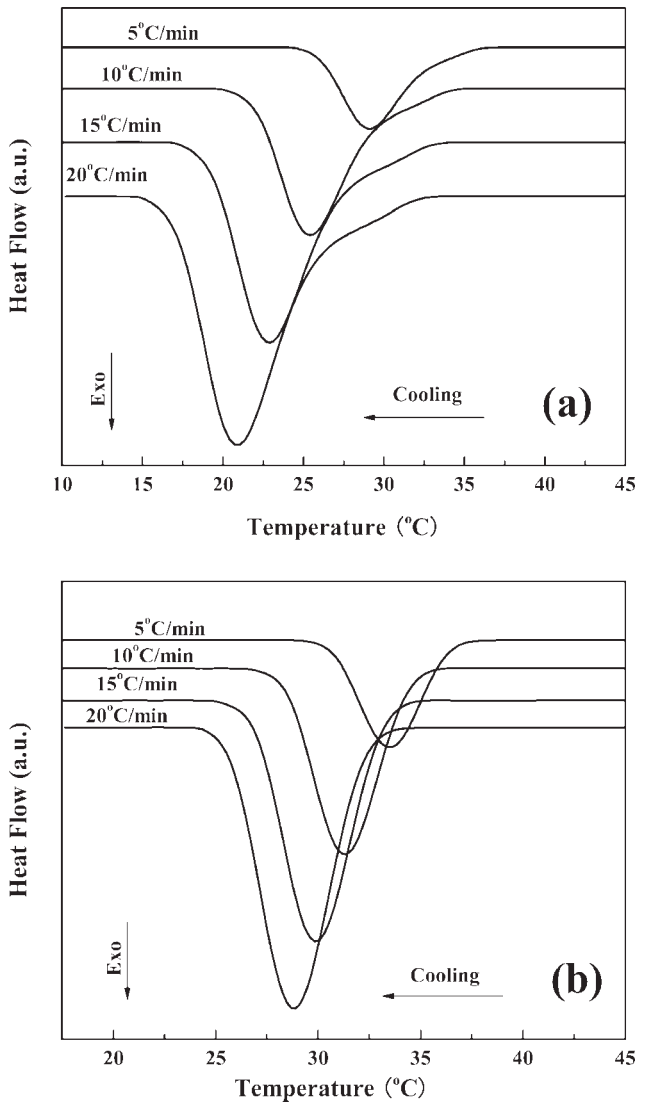

Figure 1 DSC curves of the nonisothermal melt crystallization of (a) neat PCL and (b) the 98/2 PCL/LDH nanocomposite at the indicated cooling rates.

crystallization exotherms of neat PCL and the 98/2 PCL/LDH nanocomposite (as an example). From these curves, the values of the crystallization peak temperature (T_p) and the onset temperature of crystallization (T_0) at different cooling rates were obtained, and they are listed in Table I. For all the samples, both T_0 and T_p shifted to lower temperatures and the crystallization peak became broader with the cooling rate, and this indicated that at lower cooling rates, crystallization occurred earlier or at a higher temperature. When the samples were cooled quickly from the melt, the motion of the PCL chains could not follow the cooling rate. Therefore, higher supercooling was required to initiate crystallization at a higher cooling rate.[24–26] Also, we can conclude from Figure 1 and Table I that at a fixed cooling rate, the T_p values of PCL/LDH nanocomposites with different LDH loadings were higher than that of neat PCL. This can be explained by the theory proposed by Ebengou.[27] The LDH nanoparticles had a heterogeneous nucleation effect on the PCL chain segments, which could be easily attached to the surface of the LDH nanoparticles. As a result, the crystallization of PCL was promoted and occurred at a higher crystallization temperature. However, at the cooling rates of 5 and 20°C/min, T_p of the 96/4 PCL/LDH nanocomposite was slightly lower than that of the 98/2 PCL/LDH nanocomposite. This can be attributed to the restriction against the PCL chain motion caused by too many LDH nanoparticles.

Nonisothermal crystallization kinetics

To further analyze the nonisothermal crystallization process, the crystallization kinetics of neat PCL and PCL/LDH nanocomposites was compared. The determination of the absolute crystallinity was not required for the crystallization kinetics analysis. The relative crystallinity (X_t) as a function of temperature can be defined as follows:

$$X_t = \int_{T_0}^{T} \left(\frac{dH_c}{dT}\right) dT \Big/ \int_{T_0}^{T_\infty} \left(\frac{dH_c}{dT}\right) dT \qquad (1)$$

where T_∞ is the end temperature of crystallization and dH_c/dT is the heat flow rate. The development of X_t with the crystallization temperature at various cooling rates is presented in Figure 2. All the curves show a similar sigmoid, so only the thermal lag effect of the cooling rate on crystallization can be observed from these curves. That is, melt crystallization occurred at a higher temperature with a lower cooling rate and occurred at a lower temperature

TABLE I
Values of T_p, t_{Tp}, and $X_{t,Tp}$ at the Maximum Rate of Heat Flow During the Nonisothermal Melt Crystallization of Neat PCL and PCL/LDH Nanocomposites

Sample	Φ (°C/min)	T_p (°C)	t_{Tp} (min)	$X_{t,Tp}$ (%)	$t_{1/2}$ (min)
Neat PCL	5	29.1	1.36	56.9	1.30
	10	25.4	0.95	58.4	0.90
	15	22.9	0.69	59.2	0.65
	20	21.0	0.58	57.9	0.55
99/1 PCL/LDH	5	33.4	0.85	52.3	0.83
	10	31.3	0.49	51.1	0.49
	15	29.8	0.36	53.7	0.35
	20	28.9	0.28	50.0	0.27
98/2 PCL/LDH	5	34.4	0.87	53.5	0.85
	10	31.8	0.56	58.9	0.52
	15	30.3	0.39	58.4	0.37
	20	29.3	0.30	56.5	0.28
96/4 PCL/LDH	5	34.3	0.99	58.0	0.94
	10	32.0	0.51	53.3	0.50
	15	30.6	0.38	50.0	0.38
	20	29.3	0.30	53.0	0.29

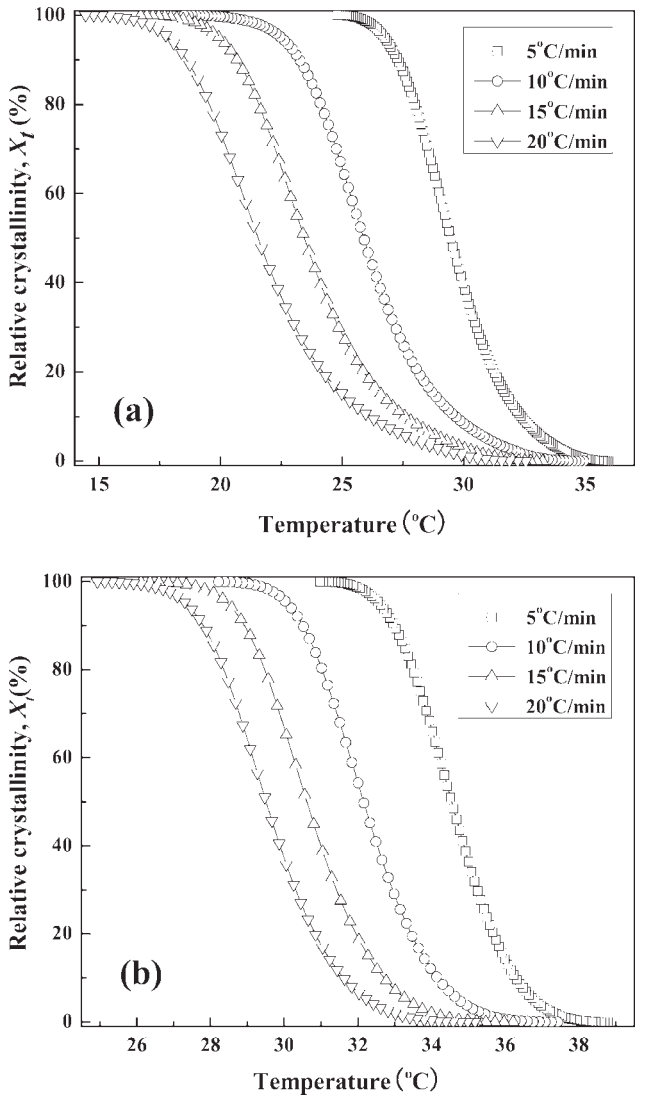

Figure 2 Development of X_t with temperature for the nonisothermal melt crystallization of (a) neat PCL and (b) the 98/2 PCL/LDH nanocomposite.

with a higher cooling rate. In general, at lower cooling rates, there is sufficient time to activate nucleation at higher temperatures.[28]

During the nonisothermal melt crystallization process, the relationship between crystallization time t and crystallization temperature T can be described as follows:

$$t = (T_0 - T)/\Phi \tag{2}$$

where Φ is the cooling rate. According to eq. (2), the value of T on the x axis in Figure 2 can be transposed into t, as shown in Figure 3. The relative crystallinity at T_p ($X_{t,Tp}$) and the crystallization time at T_p (t_{Tp}) at different cooling rates are shown in Table I. The value of $X_{t,Tp}$ changed randomly between 50 and 60%. As the cooling rate became faster, t_{Tp} became lower. This indicates that the crystallization of neat PCL and PCL/LDH nanocomposites occurred at a higher temperature and took more time as the cooling rate decreased, and this implies that the crystallization was controlled by the nucleation process.[26]

The crystallization half-time ($t_{1/2}$) is defined as the time taken from the onset of crystallization to the time when X_t is 50%:

$$t_{1/2} = \frac{T_0 - T_{1/2}}{\Phi} \tag{3}$$

where $T_{1/2}$ is the crystallization temperature corresponding to the X_t value of 50%. The $t_{1/2}$ values of neat PCL and PCL/LDH nanocomposites are also listed in Table I. $t_{1/2}$ became higher as the cooling rate increased, and this also indicates that neat PCL and its LDH nanocomposites crystallized faster when the cooling rate was higher. The crystallization

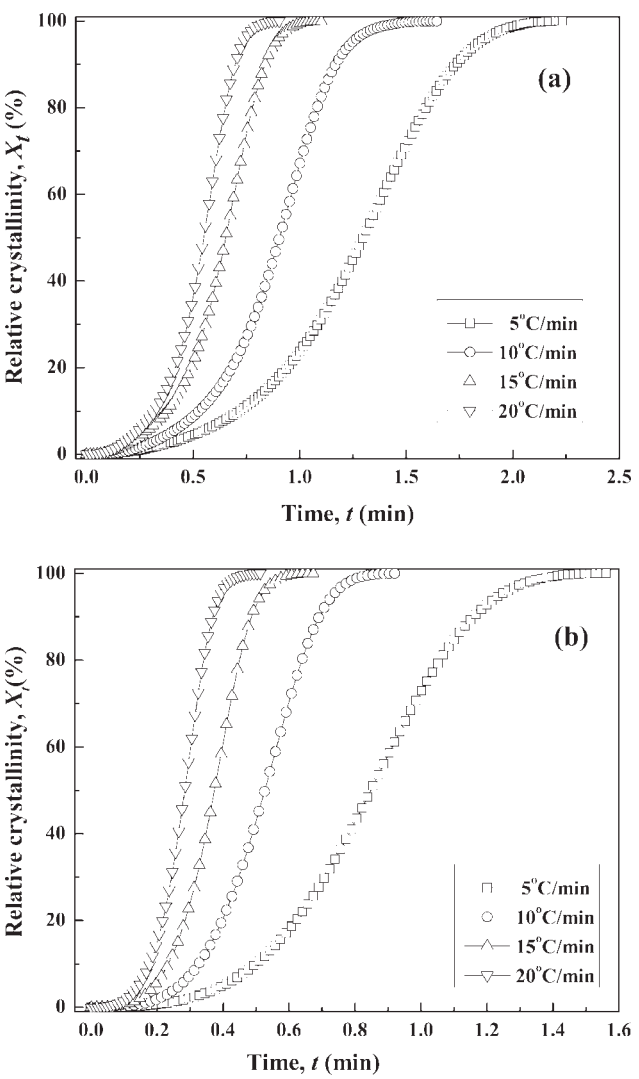

Figure 3 X_t versus time during the nonisothermal melt crystallization of (a) neat PCL and (b) the 98/2 PCL/LDH nanocomposite.

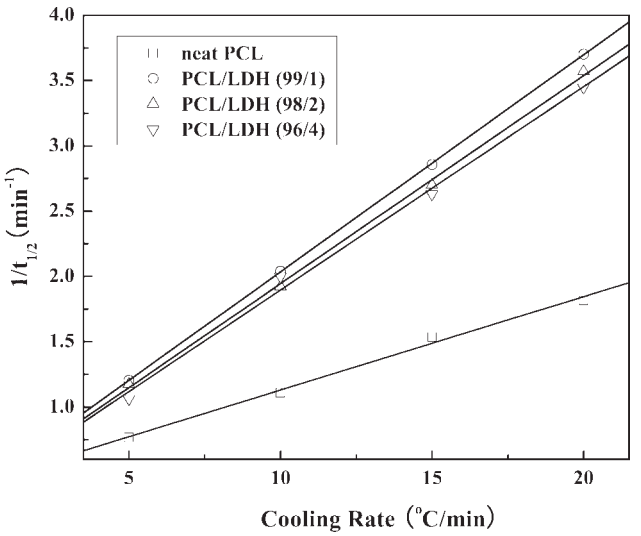

Figure 4 Plots of $1/t_{1/2}$ versus the cooling rate for neat PCL and its nanocomposites with different LDH contents.

rate parameter (CRP)[29–31] is used to quantitatively compare nonisothermal crystallization rates, which can be determined from the slope of a line in a plot of $1/t_{1/2}$ versus the cooling rate. The faster the crystallization rate is, the higher the slope is. Figure 4 shows plots of $1/t_{1/2}$ as a function of the cooling rate, and the CRP values and correlation coefficients of the nonisothermal melt crystallization of neat PCL and PCL/LDH nanocomposites are listed in Table II. From the CRP values in Table II, we can see that the crystallization rate increased when LDH nanoparticles were added to the PCL matrix. However, the CRP value decreased with an increase in the loading of LDH nanoparticles. These results imply that LDH nanoparticles could act as heterogeneous nucleating agents to facilitate the overall crystallization, whereas more LDH nanoparticles could lead to a higher interfacial area and interactions between the polymer matrix and the LDH nanoparticles, which would reduce the mobility of polymer chain segments, as observed in polymer/clay nanocomposites.[31,32]

To get a full understanding of crystallization during nonisothermal crystallization, the Ozawa, Avrami, and combined Avrami–Ozawa methods were used to analyze the nonisothermal crystallization kinetics of PCL and PCL/LDH nanocomposites.

Ozawa method

Ozawa[33] considered the nonisothermal crystallization process to be a result of infinitesimally small isothermal crystallization steps. According to this theory, nonisothermal crystallization is a rate-dependent process. Thus, X_t can be written as a function of Φ:

$$1 - X_t = \exp\left[-\frac{K(T)}{\Phi^m}\right] \tag{4}$$

where $K(T)$ is a cooling function and m is the Ozawa exponent, which depends on the crystal growth and nucleation mechanism. According to eq. (4), a double logarithmic form can be written as follows:

$$\ln[-\ln(1 - X_t)] = \ln K(T) - m \ln \Phi \tag{5}$$

Based on eq. (5), Ozawa plots of $\ln[-\ln(1 - X_t)]$ versus $\ln \Phi$ for PCL and its LDH nanocomposites are shown in Figure 5. If the Ozawa method is valid, the plot of $\ln[-\ln(1 - X_t)]$ versus $\ln \Phi$ at a fixed temperature should be linear, and as a result, $K(T)$ and m can be obtained from the slope and the intercept, respectively. As can be seen in Figure 5, the plot of neat PCL shows a better linear relationship [Fig. 5(a)], whereas curves are found in the plots of the PCL/LDH nanocomposite [Fig. 5(b)]. The continuous change in the slope indicates that m is not constant with temperature, and cooling function $K(T)$ cannot be determined because of the curvature present in the curves of the nanocomposite. This is probably due to the ignorance of secondary crystallization, the dependence of the fold length on temperature, and the constant value of the cooling function over the entire crystallization process in the Ozawa theory.[34,35] Therefore, the Ozawa method is not an effective way of describing PCL/LDH nanocomposites.

Avrami method

A generally accepted model for studying the crystallization kinetics of polymers is the Avrami theory:[36,37]

$$1 - X_t = \exp(-Z_t t^n) \quad \text{or} \quad \ln[-\ln(1 - X_t)] = \ln Z_t + n \ln t \tag{6}$$

where Avrami exponent n is a mechanism constant that depends on the type of nucleation and growth and parameter Z_t is a composite rate constant involving both nucleation and growth rate parameters. n and Z_t have an explicit physical meaning for

TABLE II
CRP and Correlation Coefficient (R) Values of the Nonisothermal Melt Crystallization of Neat PCL and PCL/LDH Nanocomposites

	Sample			
	Neat PCL	99/1 PCL/LDH	98/2 PCL/LDH	96/4 PCL/LDH
CRP	0.071	0.166	0.159	0.156
R	0.99713	0.99998	0.99939	0.99744

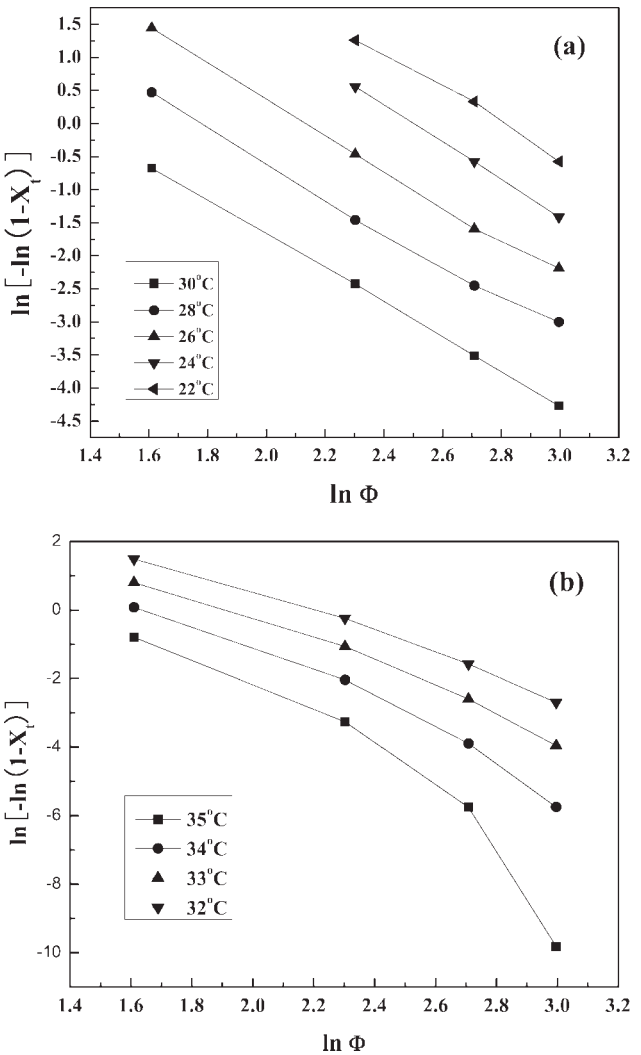

Figure 5 Ozawa plots of ln[−ln(1 − X_t)] versus ln Φ for the nonisothermal melt crystallization of (a) neat PCL and (b) the 98/2 PCL/LDH nanocomposite.

isothermal crystallization, but for nonisothermal crystallization, their physical meaning does not have the same significance because of the constant change in temperature. Thus, this must affect both nucleation and crystal growth processes because they are both temperature-dependent. Under such circumstances, therefore, n and Z_t are only two adjustable parameters to be fitted to the data obtained from the nonisothermal crystallization process. Although the physical meaning of n and Z_t cannot be related in a simple way to the isothermal case, the direct application of eq. (6) could still provide some insights into the description of the nonisothermal crystallization kinetics of many polymeric systems.[38,39] Considering the nonisothermal character of the investigated crystallization process, Jeziorny[40] pointed out that the value of rate parameter Z_t should be adequately corrected. The factor that should be considered is Φ. Under the assumption of a constant or approximately constant value of Φ, the final form of the parameter characterizing the kinetics of nonisothermal crystallization can be presented as follows:

$$\ln Z_c = \frac{\ln Z_t}{\Phi} \tag{7}$$

where Z_t is the crystallization rate parameter and Z_c is the modified crystallization rate parameter with respect to cooling rate, Φ.

The values of Avrami exponent n and rate parameter Z_t can be determined from the slope and intercept of a plot of ln[−ln(1 − X_t)] versus ln t, respectively. Plots of ln[−ln(1 − X_t)] versus ln t for PCL and its nanocomposites are shown in Figure 6, and the results are also listed in Table III. The average values of n were about 3.9, 3.6, 3.4, and 3.5 for neat PCL, 99/1 PCL/LDH, 98/2 PCL/LDH, and 96/4 PCL/LDH, respectively. On the basis of the n value

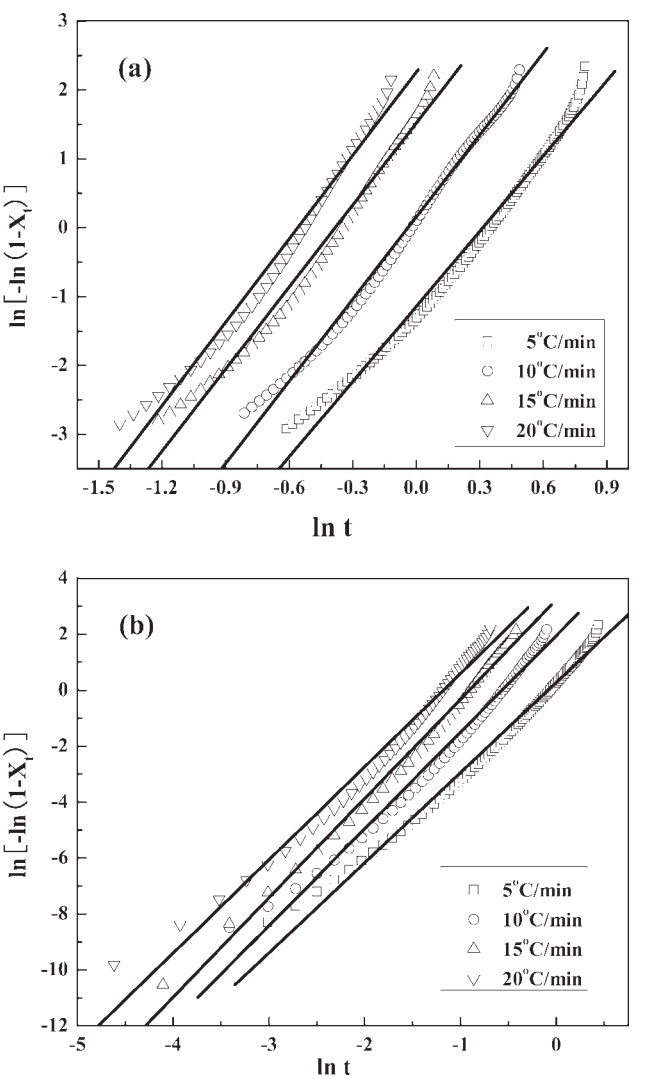

Figure 6 Plots of ln[−ln(1 − X_t)] versus ln t for the nonisothermal melt crystallization of (a) neat PCL and (b) the 98/2 PCL/LDH nanocomposite.

TABLE III
Effect of Φ on the Crystallization Kinetic Parameters of the PCL/LDH Nanocomposites

Sample	Φ (°C/min)	n	Z_t
Neat PCL	5	3.6	0.32
	10	4.0	1.17
	15	4.0	4.56
	20	4.0	9.58
99/1 PCL/LDH	5	3.2	1.31
	10	3.7	10.33
	15	3.7	32.32
	20	3.6	73.66
98/2 PCL/LDH	5	3.2	1.32
	10	3.5	7.07
	15	3.5	25.18
	20	3.3	50.36
96/4 PCL/LDH	5	3.3	0.90
	10	3.2	6.93
	15	3.6	21.43
	20	4.2	67.15

of neat PCL, its nucleation type should predominantly be homogeneous thermal nucleation, and its crystal growth is three-dimensional spherulitic growth. The values of n for the PCL/LDH nanocomposites were lower than that for neat PCL; however, the values were still higher than 3. These results indicate that the crystal growth of PCL is still three-dimensional, whereas the process of crystallization is less time-dependent. Therefore, it can be concluded that LDH nanoparticles act as nucleating agents and induce a typical heterogeneous nucleation mechanism during the crystallization of PCL/LDH nanocomposites.

Combined Avrami–Ozawa method

To describe the nonisothermal crystallization process more efficiently, a combined model proposed in our previous work was used here for comparison. The kinetic equation was deduced by the combination of the Avrami equation with the Ozawa equation, and thus a novel equation was obtained:[41]

$$\ln Z_t + n \ln t = \ln K(T) - m \ln \Phi \tag{8}$$

This can be rearranged into the following equation at a fixed value of X_t:

$$\ln \Phi = \ln F(T) - \alpha \ln t \tag{9}$$

where the parameter $F(T) = [K(T)/Z_t]^{1/m}$ refers to the value of the cooling rate, which has to be chosen at the unit crystallization time when the measured system amounts to a given degree of crystallinity. This means that $F(T)$ has a definite physical and practical meaning for nonisothermal crystallization processes, just as Z_t does for the isothermal case. α is the ratio of Avrami exponent n to Ozawa exponent m (i.e., $\alpha = n/m$). Based on eq. (9), plots of ln Φ versus ln t at a given value of X_t are shown in Figure 7 and exhibit a good linear relationship; this suggests that this analysis method is more effective in describing the nonisothermal crystallization kinetics of PCL and its LDH nanocomposites.

Kinetic parameter $F(T)$ and exponent α can be obtained from the intercept and slope of plots of ln Φ versus ln t, respectively. The values of $F(T)$ and α at given values of X_t are listed in Table IV. The value of $F(T)$ increased as X_t became higher, and this indicates that at the unit crystallization time, a higher X_t value could be obtained with a higher cooling rate. In addition, the values of $F(T)$ for the PCL/LDH nanocomposites were lower than that for neat PCL at the same X_t value, and this suggests that the addition of LDH nanoparticles accelerated the crystal growth process of PCL. However, the

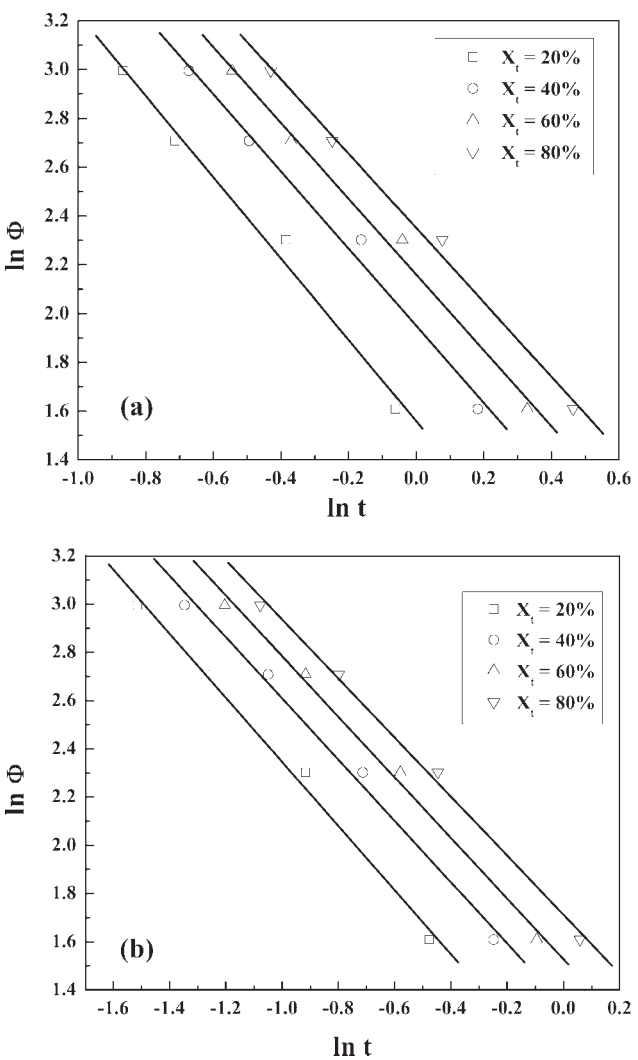

Figure 7 Plots of ln Φ versus ln t for the nonisothermal melt crystallization of (a) neat PCL and (b) the 98/2 PCL/LDH nanocomposite.

TABLE IV
Nonisothermal Crystallization Kinetic Parameters with Different X_t Values by the Avrami–Ozawa Combination Method

Sample		X_t (%)			
		20	40	60	80
Neat PCL	$F(T)$	4.754	7.028	8.675	10.498
	α	1.7	1.6	1.6	1.5
99/1 PCL/LDH	$F(T)$	2.683	3.662	4.435	5.449
	α	1.3	1.2	1.3	1.2
98/2 PCL/LDH	$F(T)$	2.760	3.812	4.599	5.534
	α	1.3	1.3	1.3	1.2
96/4 PCL/LDH	$F(T)$	3.425	4.219	4.919	5.645
	α	1.2	1.2	1.2	1.2

more LDH nanoparticles were in the composites, the higher $F(T)$ was, and this indicates that a higher LDH loading hinders the motion of PCL chains and the melt crystallization process. For the sample with the same LDH loading, the values of α showed only a slight variation at different X_t values, and this indicates that the mechanism of nucleation and growth remained the same as X_t changed. Moreover, the α value of neat PCL (ca. 1.6) differed obviously from that of PCL nanocomposites with different LDH loadings (ca. 1.2), and this suggests that the addition of LDH greatly affected the nucleation and growth mechanism of PCL. Besides, the α value did not change much as more LDH nanoparticles were added to the PCL matrix, and this indicates that the loading level of LDH did not change the mechanism of nonisothermal crystallization for the PCL nanocomposites.

Obviously, the Ozawa–Avrami combination method can effectively describe the nonisothermal crystallization kinetics of PCL/LDH nanocomposites. The advantage of the combined kinetic model is that it correlates the cooling rate to the temperature, time, and morphology (i.e., nucleation and growth mechanism of crystals). This combined kinetic method has also been proved to be effective in many other polymeric and polymer nanocomposite systems, such as poly(ether ether ketone ketone),[41] poly(oxybiphenyl-4,4′-diyloxy-1,4-phenylenecarbonyl-1,3-phenylenecarbonyl-1,4- phenylene) (PEDEKmK),[42] poly(ethylene 2,6-naphthalate),[43] poly(3-dodecylthiophene),[44] poly(ethylene terephthalate)/antimony-doped tin oxide nanocomposites,[45] polypropylene/silica nanocomposites,[46] high-density polyethylene/polyhedral oligomer silsesquioxane nanocomposites,[35] nylon 11/ZnO composites,[47] polypropylene/LDH nanocomposites,[48] and nylon 6/clay nanocomposites.[32]

Crystallization activation energy (ΔE)

It is important to evaluate ΔE for nonisothermal crystallization. Among the commonly used methods, the Kissinger method[49] has been one of the most popular approaches for evaluating nonisothermal ΔE values. However, Vyazovkin[50] demonstrated that this method is inappropriate for melt crystallization. Therefore, the Takhor model[51] was used here to estimate ΔE for the transport of polymer chains toward the growing surface. According to the Takhor model, ΔE can be determined with the following equation:

$$\frac{d[\ln(\Phi)]}{d(1/T_p)} = -\frac{\Delta E}{R} \tag{10}$$

where R is the universal gas constant. The plots obtained from the Takhor model are shown in Figure 8. ΔE was calculated from the slope (i.e., $\Delta E = -R \times$ slope), and the results are listed in Table V.

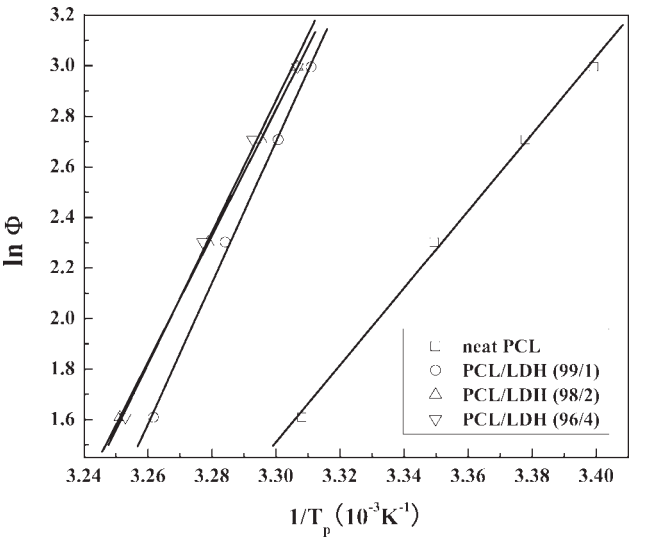

Figure 8 Plots for estimating the activation energy of nonisothermal melt crystallization with the Takhor model.

As can be seen in Table V, all the values of ΔE were negative, and this indicates that the crystallization is a heat-releasing process. Here we introduce $|\Delta E|$ as the absolute value of ΔE for convenience. The higher $|\Delta E|$ is, the more heat has to be released for crystallization. The $|\Delta E|$ value of neat PCL was lower than the values of its LDH nanocomposites, and this indicates that it was more difficult for PCL to crystallize in the presence of LDH nanoparticles. This should be attributed to the reduction of the transportability of polymer chains caused by the addition of LDH. Although the addition of LDH would cause a heterogeneous nucleation effect, the

TABLE V
Values of ΔE Calculated with the Takhor Model

	Sample			
	Neat PCL	99/1 PCL/LDH	98/2 PCL/LDH	96/4 PCL/LDH
ΔE (kJ/mol)	−126.6	−232.1	−207.4	−216.4

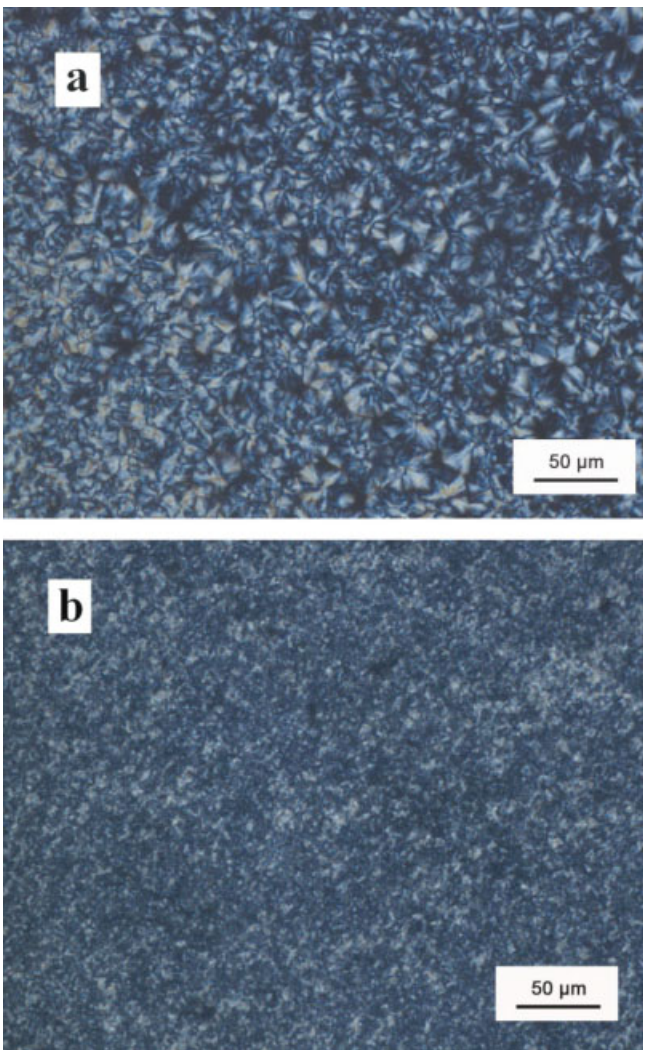

Figure 9 POM micrographs of (a) neat PCL and (b) the 96/4 PCL/LDH nanocomposite (both nonisothermally melt-crystallized). [Color figure can be viewed in the online issue, which is available at www.interscience.wiley.com.]

hindrance effect of LDH seemed not to be neglected. When a small amount of LDH nanoparticles (e.g., 1 wt %) was added, the mobility of PCL chains decreased. As the amount of LDH was small, its heterogeneous effect was not that obvious, and thus the $|\Delta E|$ value of the nanocomposites was higher than that of neat PCL. When the amount of LDH was increased to a certain extent (e.g., 2 wt %), the mobility of PCL chains became even lower despite the heterogeneous effect of LDH. As a result, the value of $|\Delta E|$ decreased as the amount of LDH increased to a certain degree. However, when the amount of LDH exceeded a certain amount (e.g., 4 wt %), the mobility of PCL chains was restricted even more significantly, and this led to an even higher potential barrier to be overcome to achieve the structural arrangement of PCL chains during the melt crystallization process. Accordingly, $|\Delta E|$ was even higher as the LDH content was further increased above a certain amount.

Spherulitic growth behavior

Figure 9 shows POM photographs of neat PCL and its nanocomposite with 4 wt % LDH. The size of the PCL spherulites decreased upon the incorporation of LDH into the matrix. This phenomenon was attributed to the nucleation effect of the LDH nanoparticles, which provided much more heterogeneous nuclei and reduced the size of the spherulites. Because of the impingement effect, it was hard to form perfect or well-developed spherulites when the LDH content was high. The presence of a large number of heterogeneous nuclei (i.e., LDH nanoparticles) resulted in restricted growth of numerous but small PCL spherulites. Therefore, it can be concluded that the presence of LDH and its content in the matrix apparently influence the spherulitic size and overall crystallization process of PCL. This is in good agreement with the nonisothermal crystallization behavior observed from DSC results.

CONCLUSIONS

The nonisothermal melt crystallization kinetics of PCL and its LDH nanocomposites was investigated by a DSC technique at different cooling rates. The Avrami equation, the Ozawa method, and the combined Avrami–Ozawa approach were used to describe the nonisothermal crystallization behavior. The Ozawa method failed to describe the nonisothermal crystallization behavior of PCL nanocomposites, probably because of the inaccurate assumption of the Ozawa theory. The Avrami analysis was used to explain the crystallization kinetics for these systems, but the parameters could not give us explicit meaning for nonisothermal crystallization. The combined kinetic method was able to satisfactorily describe the nonisothermal crystallization behavior of PCL and its LDH nanocomposites. The analysis of the crystallization process showed that the addition of LDH nanoparticles accelerated the growth of PCL crystallization. The activation energy for nonisothermal crystallization was evaluated with the Takhor model. Compared with that of neat PCL, the activation energy of the LDH nanocomposites was higher because of the hindrance effect of the nanoparticles. Different kinetic parameters obtained from these models have proved that LDH nanoparticles added to the PCL matrix play two competing roles: on the one hand, they are a heterogeneous nucleation medium promoting the crystallization process of PCL; on the other hand, they physically hinder polymer chain mobility and thus retard the crystal growth process of PCL.

References

1. Gilman, J. W. Appl Clay Sci 1999, 15, 31.
2. Decker, L. C.; Zahouily, K.; Keller, L.; Benfarhi, S.; Bendaikha, T.; Baron, J. J Mater Sci 2002, 37, 4821.
3. Alexandre, M.; Dubois, P. Mater Sci Eng R 2000, 28, 1.
4. Newman, S. P.; Jones, W. New J Chem 1998, 22, 105.
5. Sideris, P. J.; Nielsen, U. G.; Gan, Z. H.; Grey, C. P. Science 2008, 321, 113.
6. Zammarano, M.; Bellayer, S.; Gilman, J. W.; Franceschi, M.; Beyer, F. L.; Harris, R. H.; Meriani, S. Polymer 2006, 47, 652.
7. Leroux, F.; Meddar, L.; Mailhot, B.; Morlat-Therias, S.; Gardette, J.-L. Polymer 2005, 46, 3571.
8. Costa, F. R.; Abdel-Goad, M.; Wangenknechat, U.; Heinrich, G. Polymer 2005, 46, 4447.
9. Mangiacapra, P.; Raimondo, M.; Tammaro, L.; Vittoria, V. Biomacromolecules 2007, 8, 773.
10. Gorrasi, G.; Vittoria, V.; Pollet, E.; Alexandre, M.; Dubois, P. J Polym Sci Part B: Polym Phys 2004, 42, 1466.
11. John, J.; Tang, J.; Yang, Z.; Bhattacharya, M. J Polym Sci Part A: Polym Chem 1997, 35, 1139.
12. Liao, L.; Zhang, C.; Gong, Q. Macromol Rapid Commun 2007, 28, 1148.
13. Tammaro, L.; Tortora, M.; Vittoria, V.; Costantino, U.; Marmottini, F. J Polym Sci Part A: Polym Chem 2005, 43, 2281.
14. Sorentino, A.; Gorrasi, G.; Tortora, M.; Vittoria, V.; Costantino, U.; Marmottinic, F.; Padella, F. Polymer 2005, 46, 1601.
15. Pucclariello, R.; Tammaro, L.; Villani, V.; Vittoria, V. J Polym Sci Part B: Polym Phys 2007, 45, 945.
16. Romeo, V.; Gorrasi, G.; Vittoria, V. Biomacromolecules 2007, 8, 3147.
17. Costantino, U.; Bugatti, V.; Gorrasi, G.; Montanari, F.; Nocchetti, M.; Tammaro, L.; Vittoria, V. ACS Appl Mater Interfaces 2009, 1, 668.
18. Peng, H. D.; Liu, T. X.; Huang, S.; Han, Y.; Wang, W. Z.; Lai, Z. L.; Wu, P. Y.; Tjiu, W. C.; He, C. B. Thermochimica Acta 2010, to appear.
19. Lorenzo, M. L. D.; Silvestre, C. Prog Polym Sci 1999, 24, 917.
20. Wu, T. M.; Chen, E. C. Polym Eng Sci 2006, 46, 1309.
21. Liu, Q.; Peng, Z. Q.; Chen, D. J. Polym Eng Sci 2007, 47, 460.
22. Hua, L.; Kai, W. H.; Inoue, Y. J Appl Polym Sci 2007, 106, 4225.
23. Liu, Z. P.; Ma, R. Z.; Osanda, M.; Iyi, N.; Ebina, Y.; Takada, K.; Sasaki, T. J Am Chem Soc 2006, 128, 4872.
24. Xu, W. B.; Ge, M. L.; He, P. S. J Polym Sci Part B: Polym Phys 2002, 40, 408.
25. Ma, J. S.; Zhang, S. M.; Qi, Z. N.; Li, G.; Hu, Y. L. J Appl Polym Sci 2002, 83, 1978.
26. Kim, J. Y.; Park, H. S.; Kim, S. H. Polymer 2006, 47, 1379.
27. Ebengou, R. H. J Polym Sci Part B: Polym Phys 1997, 35, 1333.
28. Lopez, L. C.; Wilkes, G. L. Polymer 1989, 30, 882.
29. Zhang, R. Y.; Zheng, H. F.; Lou, X. L.; Ma, D. Z. J Appl Polym Sci 1994, 51, 51.
30. Supaphol, P.; Dangseeyun, N.; Srimoaon, P. Polym Test 2004, 23, 175.
31. Huang, J. W.; Hung, H. C.; Tseng, K. S.; Kang, C. C. J Appl Polym Sci 2006, 100, 1335.
32. Fornes, T. D.; Paul, D. R. Polymer 2003, 44, 3945.
33. Ozawa, T. Polymer 1971, 12, 150.
34. Addonizio, M. L.; Martuscelli, E.; Silvestre, C. Polymer 1987, 28, 183.
35. Joshi, M.; Butola, B. S. Polymer 2005, 45, 4953.
36. Avrami, M. J Chem Phys 1939, 7, 1103.
37. Avrami, M. J Chem Phys 1940, 8, 212.
38. Qiu, Z. B.; Ikehara, T.; Nishi, T. Polymer 2003, 44, 5429.
39. Qiu, Z. B.; Fujinami, S.; Komura, M.; Nakajima, K.; Ikehara, T.; Nishi, T. Polym J 2004, 36, 642.
40. Jeziorny, A. Polymer 1978, 19, 1142.
41. Liu, T. X.; Mo, Z. S.; Wang, S. E.; Zhang, H. F. Polym Eng Sci 1997, 37, 568.
42. Liu, T. X.; Mo, Z. S.; Zhang, H. F. J Appl Polym Sci 1998, 67, 815.
43. Kim, S. H.; Ahn, S. H.; Hirai, T. Polymer 2003, 44, 5625.
44. Liu, S. L.; Chung, T. S. Polymer 2000, 41, 2781.
45. Chen, X. L.; Li, C. Z.; Shao, W.; Liu, T. X.; Wang, L. M. J Appl Polym Sci 2008, 109, 3753.
46. Jain, S.; Goossens, H.; van Duin, M.; Lemstra, P. Polymer 2005, 46, 8805.
47. Wu, M.; Yang, G. Z.; Wang, M.; Wang, W. Z.; Zhang, W. D.; Feng, J. C.; Liu, T. X. Mater Chem Phys 2008, 109, 547.
48. Lonkar, S. P.; Morlat-Therias, S.; Caperaa, N.; Leroux, F.; Gardette, J. L.; Singh, R. P. Polymer 2009, 50, 1505.
49. Kissinger, H. E. J Res Natl Bur Stand 1956, 57, 217.
50. Vyazovkin, S. Macromol Rapid Commun 2002, 23, 771.
51. Takhor, R. L. Advances in Nucleation and Crystallization of Glasses; American Ceramics Society: Columbus, OH, 1971; p 166.